Supplementary Materials

Note S1. Battery Activation

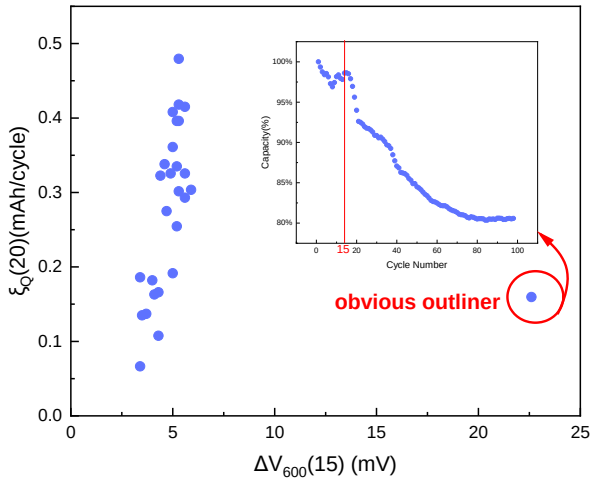


Figure S1. Example of determination of activation.

Here is an example of error made by unfinished activation. In scatter plot of ξ(20) vs ΔV_R (15), an obvious outliner can be seen. This battery's capacity curve of all cycles is plotted in the subpicture and we can find out that in this cycle this battery hasn't fully activated.

The selection of activated point is by using an algorithm to automatically choose the maximum of capacity as activated point with manual inspection and calibration. All batteries activated point can be seen in Table S1.

Note S2. Battery Voltage Derivation

$$V_{bat} = \phi_s^o - \phi_s^g \quad \text{(Equation S1)}$$

The battery voltage can be defined as the difference between solid state electrochemical potential between oxide and graphite as shown in Equation S1. For the oxide or graphite, based on the chemical reaction, the solid state electrochemical potential can be further derived as shown in Equation S2, 3. By plug in the final derivation from Equation S3 for oxide and graphite, Equation S1 can be simplified into Equation S4.

$$\mathrm{Li}^+ + e^- + V \rightarrow \mathrm{LiV}$$

$$\begin{aligned} F\eta = \Delta G &= \bar{\mu}_{LiV} - \bar{\mu}_V - \bar{\mu}_{Li^+} - \bar{\mu}_{e^-} \\ &= \mu_{LiV} - \mu_V - \left(\mu_{Li^+} + F\phi_l\right) - \left(-F\phi_s\right) \\ &= \mu_d - \mu_{Li^+} - F\phi_l + F\phi_s \end{aligned} \quad \text{(Equation S2)}$$

$$\phi_s = \frac{-\mu_d + \mu_{Li^+}}{F} + \phi_l + \eta \quad \text{(Equation S3)}$$

$$\begin{aligned} V_{bat} &= \frac{-\mu_d^o + \mu_{Li^+}^o}{F} + \phi_l^o + \eta^o - \frac{-\mu_d^g + \mu_{Li^+}^g}{F} - \phi_l^g + \eta^g \\ &= -\frac{\mu_d^o - \mu_d^g}{F} + \frac{\mu_{Li^+}^o - \mu_{Li^+}^g}{F} + \left(\phi_l^o - \phi_l^g\right) + \left(\eta^o - \eta^g\right) \end{aligned} \quad \text{(Equation S4)}$$

Note S3. Feature Formulation

The formulation for each of the features are given below.

ΔV_R is defined as:

$$\Delta V_R = V_{R,End} - V_{R,Begin} \quad \text{(Equation S5)}$$

For cycle N, the R_D is defined as:

$$R_D(N) = \frac{\int_0^1 V_{Bat}(N)\,\mathrm{dt}}{\int_0^1 I_D\,\mathrm{dt}} \quad \text{(Equation S6)}$$

Given N_1 cycle data, the prospective cumulative faraday efficiency of cycle N_2, H_{N2}, is defined as:

$$\bar{\eta}_{N_1} = \left(\prod_{i=1}^{N_1} \eta_i\right)^{1/N_1} \quad \text{(Equation S7)}$$

$$\eta_{N_2} = \left(\bar{\eta}_{N_1}\right)^{N_2} \quad \text{(Equation S8)}$$

Given N_1 cycle data, the past average capacity fade is defined as:

$$\xi_{N_1} = \frac{|C_i - C_1|}{N_1 - 1}\frac{1}{C_1} \quad \text{(Equation S9)}$$

Note S4. Dissemble of batteries classified as Slow Fading Group and Fast Fading Group

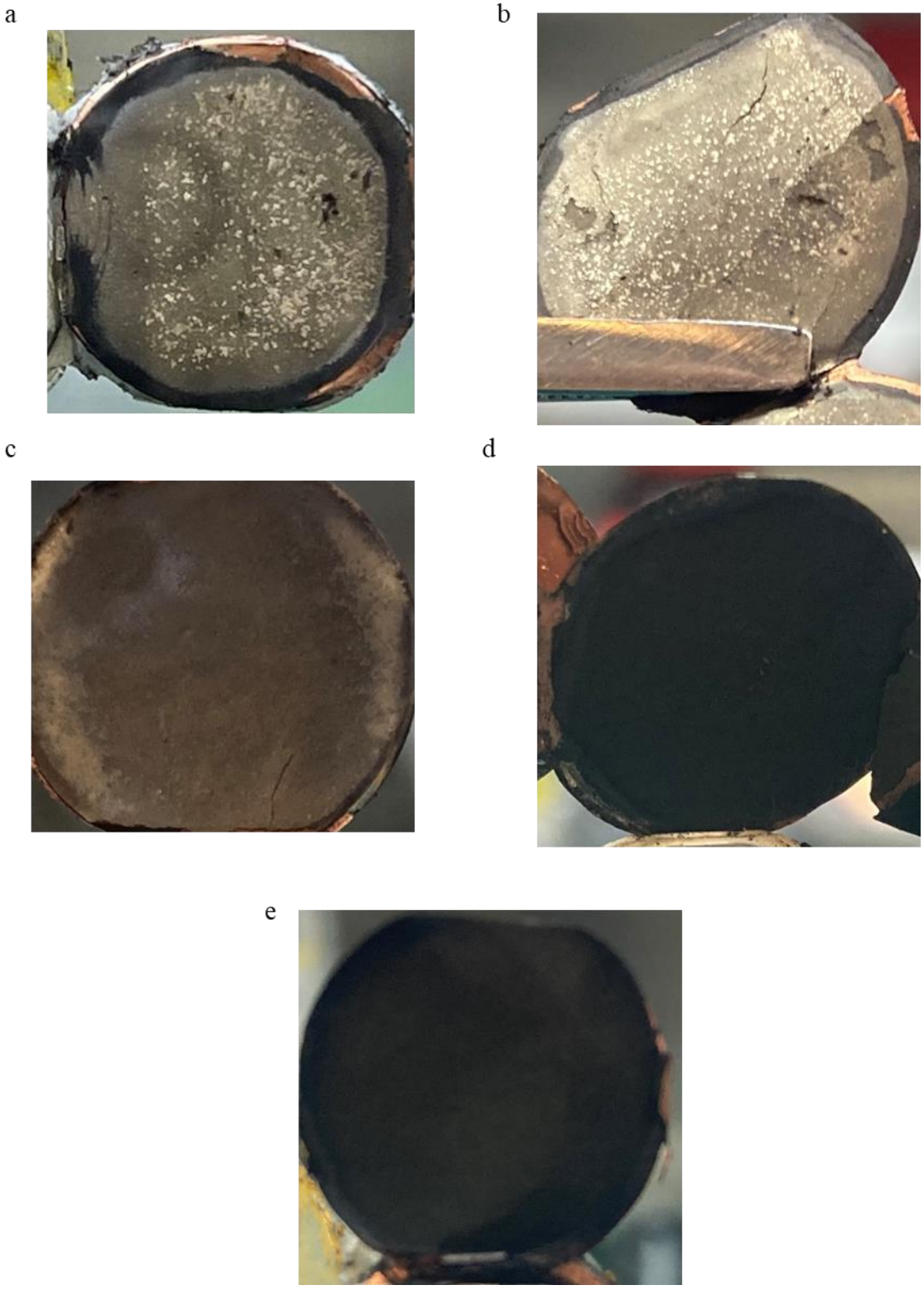
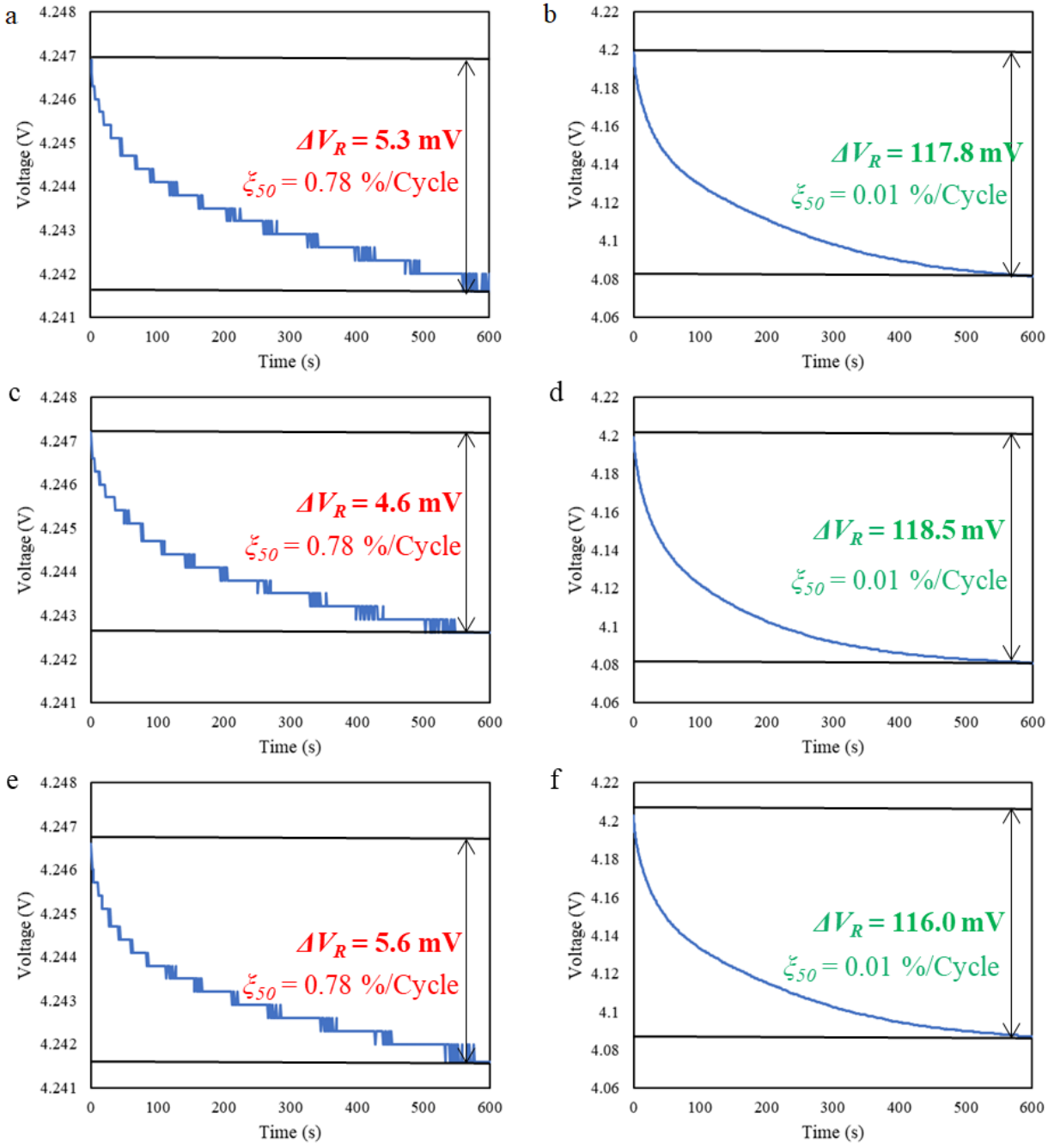


Figure S2. Example anodes of battery No. 21 (a) and No. 33 (b), classified as Fast Fading Group. The silver dots on anodes are dead Li which is caused by Li plating result in fast capacity fading rate. Example anodes

of battery No. 43 (c) and No. 25 (d), classified as Slow Fading Group, show no dead Li, (e) is the anode of a fresh cell.

Note S5. ΔV_R at Different Cycles



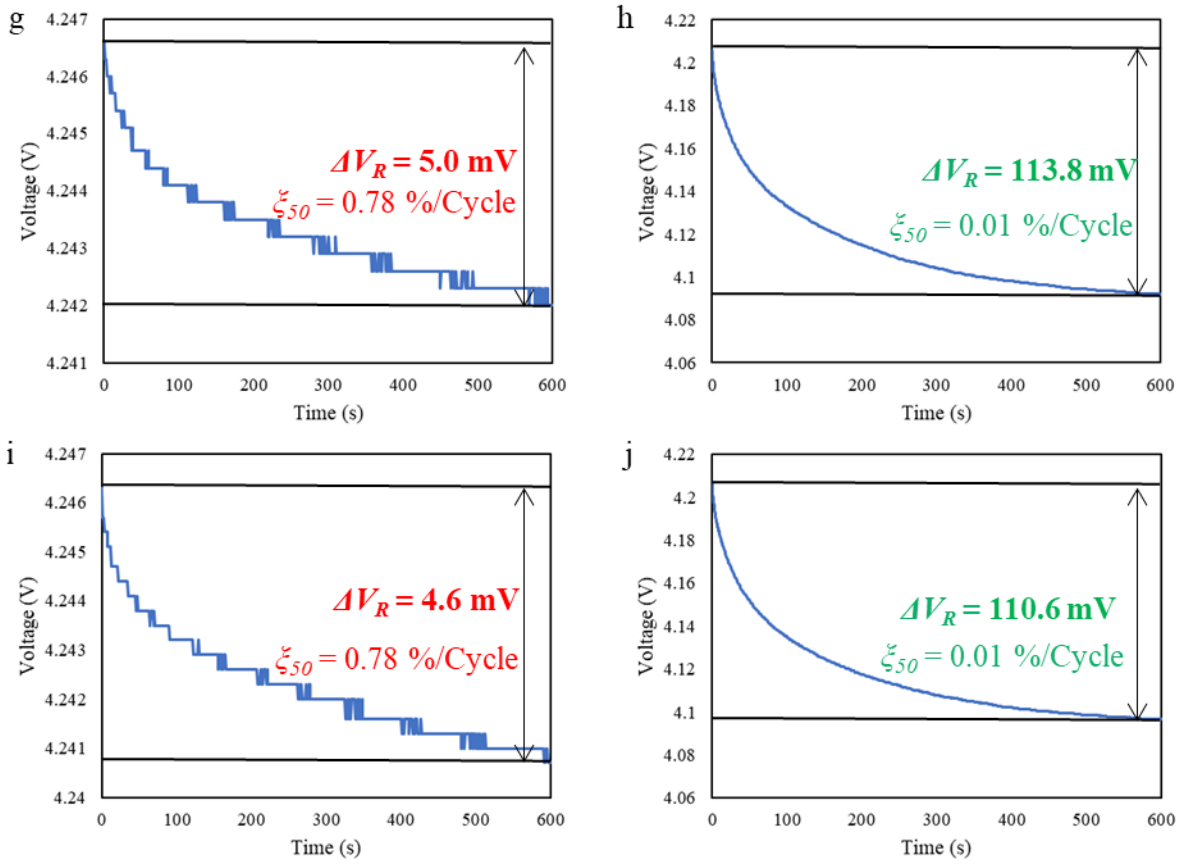


Figure. S3. ΔV_R of Battery No. 33 for 10 (a), 20 (c), 30 (e), 40 (g), and 50 (i) cycle respectively, ΔV_R of Battery No. 43 for 10 (b), 20 (d), 30 (f), 40 (h), and 50 (j) cycle respectively.

Note S6. ΔV_R for Different Batteries at Same Cycles

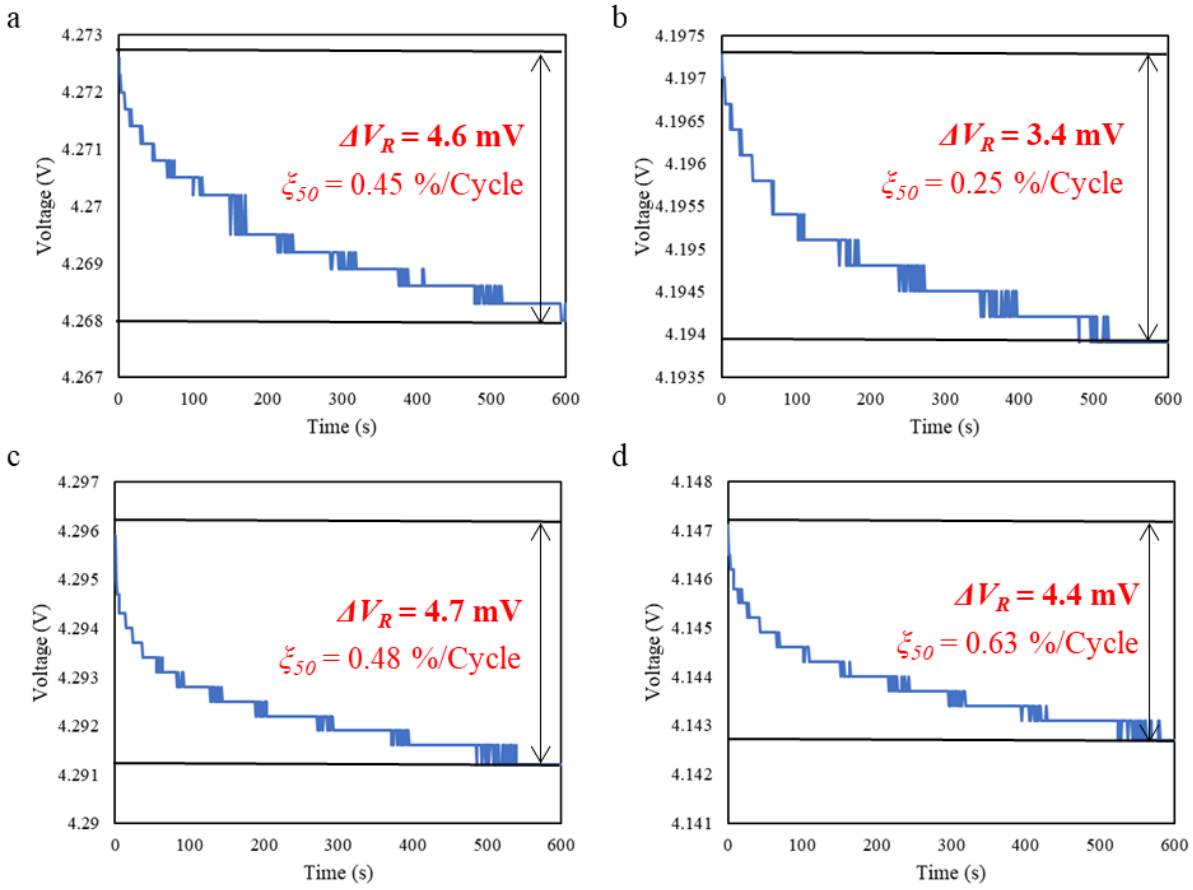


Figure S4. ΔV_R of Batteries with fast capacity fading rate at 2nd cycle. Battery 7 (a), 12 (b), 21(c), and 35 (d).

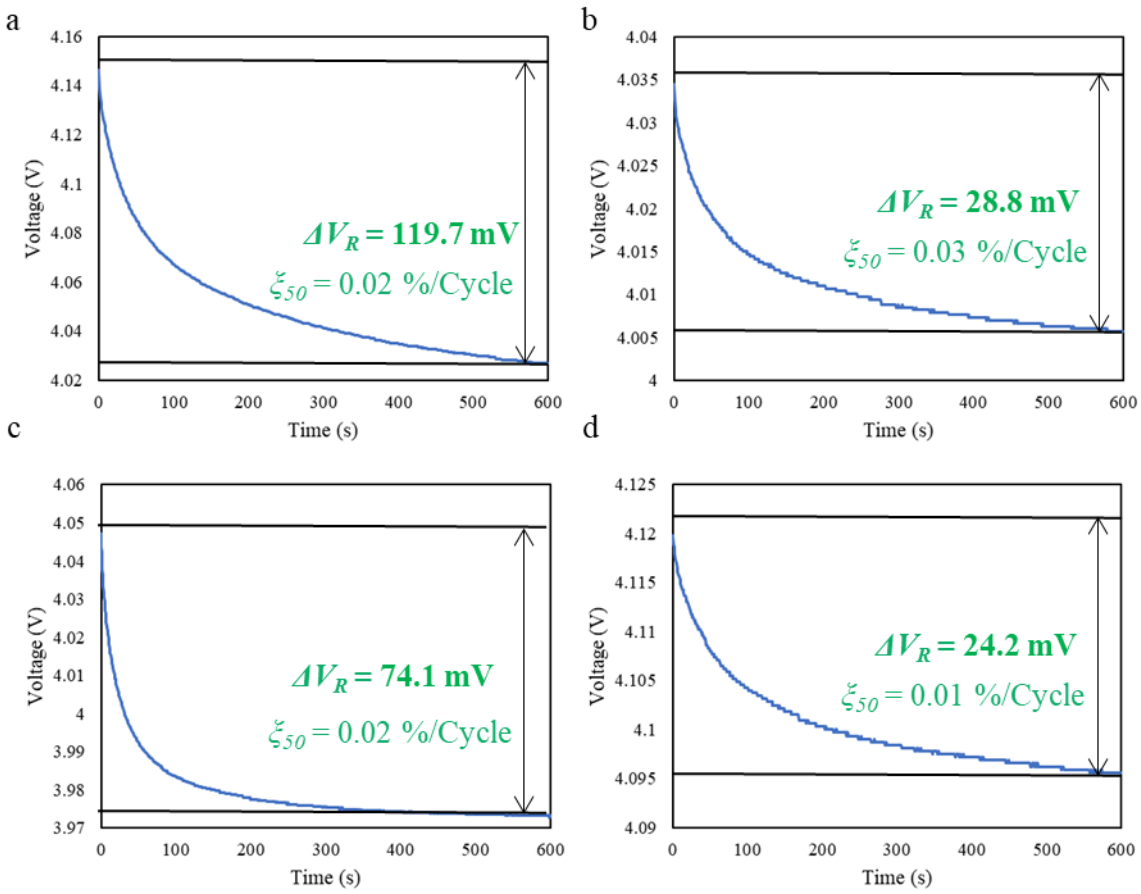


Figure S5. ΔV_R of Batteries with slow capacity fading rate at 2nd cycle. Battery 2 (a), 13 (b), 25 (c), and 40 (d).

Note S7. K-mean Clustering Results with Data Obtained from Early Cycle (1-6)

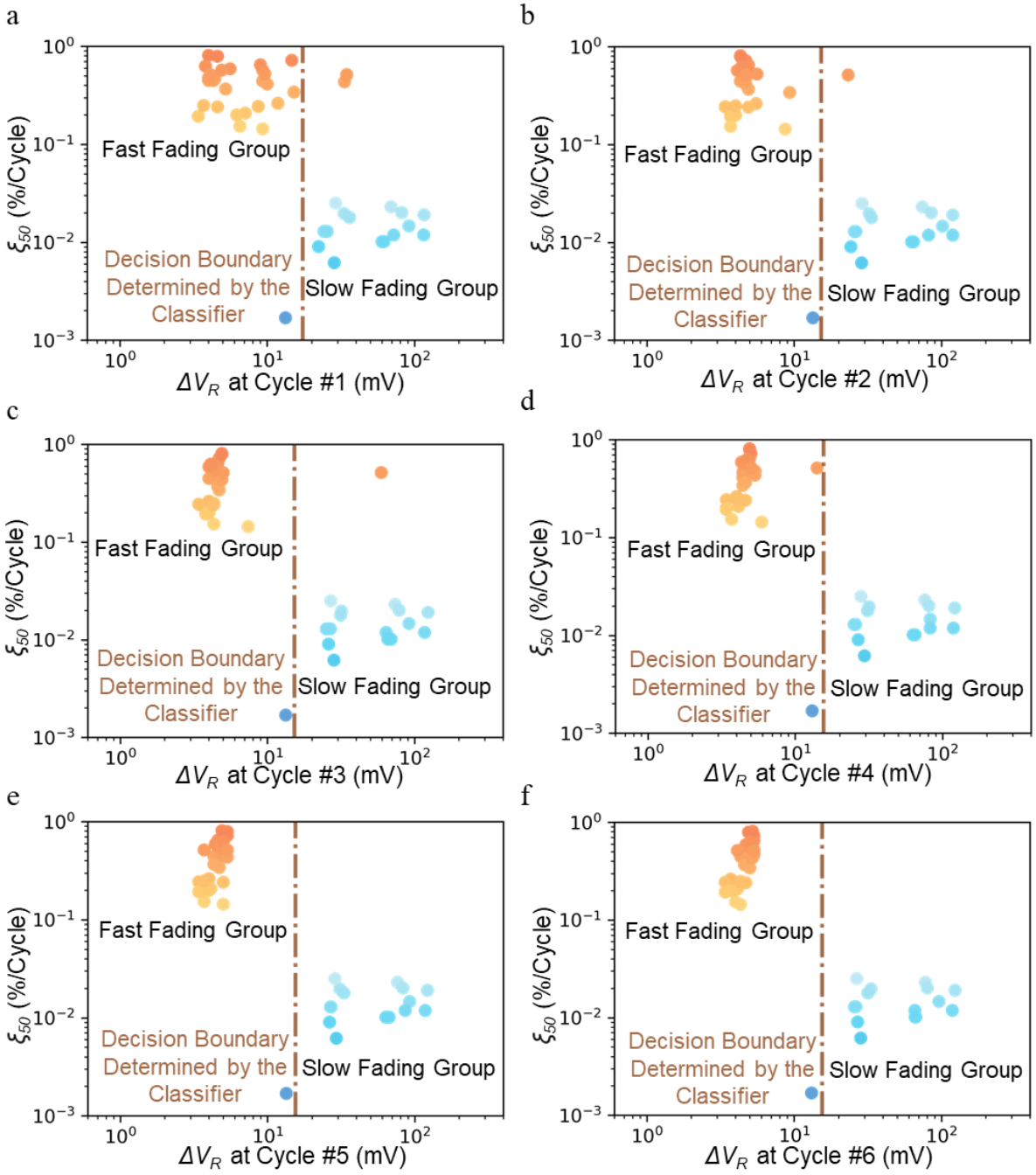


Figure S6. Clustering result with data obtained from (a) 1st cycle, (b) 2nd cycle, (c) 3rd cycle, (d) 4th cycle, (e) 5th cycle, and (f) 6th cycle.

The above figures demonstrated that physics guided feature, ΔV_R, is good indicator to classify the dominant capacity fading mechanism even with data obtained from other early cycles. With first cycling data, the clustering algorithm only misclassed 3 batteries. With 2nd and 3rd cycling data, the clustering method only make 2 mistakes. Furthermore, with 4th cycling data, the algorithm achieves only 1error.

Note S8. Evolution of ΔV_R

Compared with the SEI formation, Li plating will decrease the available capacity in a faster way leading to a harsher and harsher charging condition with fixed charging current during the cycle. To validate this statement, we demonstrate the evolution of ΔV_R for batteries with ξ_{50} > 0.1%/cycle in the first 6th cycle in Figure S7. As shown in Figure S7, at the beginning, the distribution of ΔV_R is sparse but relatively small compared to the ΔV_R of the batteries dominate by SEI growth. The sparsity indicates that even though Li plating does happen in these batteries, the Li plating reaction is not well established. Other fading mechanisms also contribute to the capacity loss. However, after 4th cycle, as the loss of active Li ion increase, the fading is dominated by Li plating therefore ΔV_R is concentrated.

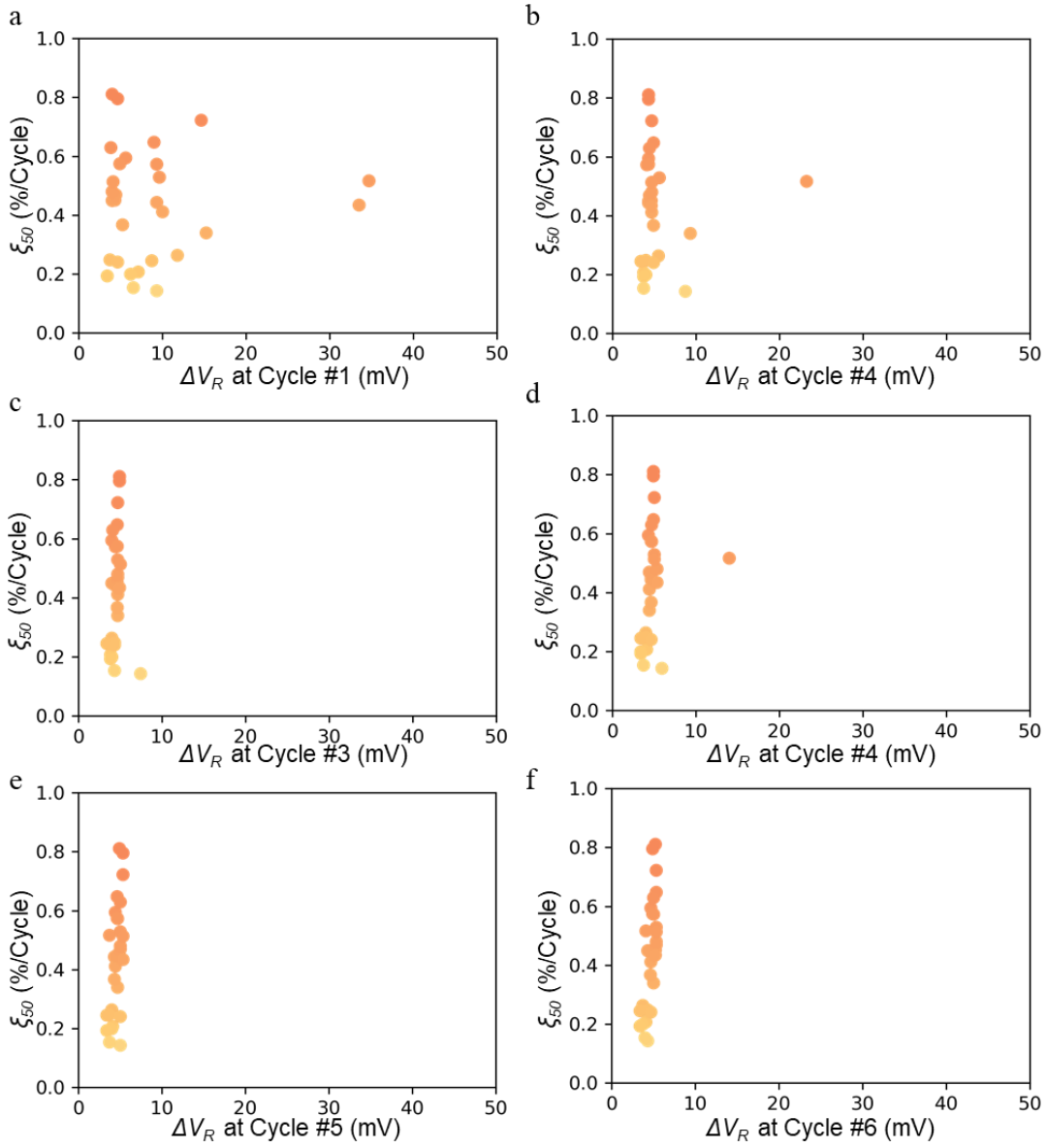


Figure S7. ΔV_R evaluation during the early cycle from sparse distribution in cycle 1 to dense distribution in cycle 6. (1-6, a-f)

Table S1. Experiment Conditions

Table S1: Experiment Conditions

Battery No.	Charging Current (mA)	C-rate	Cutoff Voltage (V)	Temperature (C)	SOC %	Activation Cycle
1	9	0.2	4.2	20	75	2
2	135	3	4.2	20	75	2
3	67.5	1.5	4.2	20	80	12
4	157.5	3.5	4.2	20	80	10
5	135	3	4.375	20	80	6
6	135	3	4.325	20	80	5
7	135	3	4.275	20	80	5
8	135	3	4.225	20	80	5
9	9	0.2	4.2	20	80	2
10	45	1	4.2	20	80	16
11	135	3	4.2	20	80	7
12	225	5	4.2	20	80	7
13	9	0.2	4.3	20	80	2
14	180	4	4.3	20	80	6
15	225	5	4.3	20	80	10
16	135	3	4.4	24	80	6
17	180	4	4.4	24	80	8
18	157.5	3.5	4.2	24	80	28
19	202.5	4.5	4.2	24	80	7
20	157.5	3.5	4.3	24	80	6
21	202.5	4.5	4.3	24	80	9
22	247.5	5.5	4.3	24	80	10
23	157.5	3.5	4.4	24	80	15
24	202.5	4.5	4.4	24	80	13
25	135	3	4.2	40	80	2
26	22.5	0.5	4.4	22	80	2
27	90	2	4.4	22	80	9
28	90	2	4.35	22	80	9
29	135	3	4.35	22	80	4
30	67.5	1.5	4.3	22	80	5
31	112.5	2.5	4.3	22	80	6
32	112.5	2.5	4.25	22	80	7
33	135	3	4.25	22	80	6
34	90	2	4.15	22	80	3
35	112.5	2.5	4.15	22	80	5
36	157.5	3.5	4.15	22	80	4
37	22.5	0.5	4.35	22	80	2

38	180	4	4.15	22	80	46
39	22.5	0.5	4.15	21	80	2
40	45	1	4.15	21	80	2
41	9	0.2	4.25	21	80	2
42	22.5	0.5	4.25	21	80	2
43	45	1	4.25	21	80	2
44	9	0.2	4.35	21	80	2
45	67.5	1.5	4.35	21	80	2

Table S2. Features Selection

Table S2: Selected Features

Model	Feature 1	Feature 2	Feature 3	Feature 4	Feature 5
Constant	Average ξ_{50} of training group*				
Univariate	Discharge Capacity at Cycle 5				
Multivariate	Slope of Discharge Capacity Cycle 1-5	Intercept of Discharge Capacity Cycle 1-5	Discharge Capacity at Cycle 1	Discharge Capacity at Cycle 5	Lost Capacity at Cycle 5
Random Forest Regression	Voltage Drop after Charing at Cycle 5 (ΔV_R)	R_D at Cycle 5	Prospective Faraday Efficiency	Average Capacity Fading rate at Cycle 5 (ξ_5)	

* Constant model use the average ξ_{50} of training group to make prediction.

Table S3. Models Performance

Model	Mean Train MAPE (%)	Standard Devidation of Train MAPE (%)	Mean Train RMSE (%/Cycle)	Standard Devidation of Train RMSE(%)	Mean Test MAPE (%)	Standard Devidation of Test MAPE (%)	Mean Test RMSE (%/Cycle)	Standard Devidation of Test RMSE(%)
Constant	703.28	64.47	0.25	0.01	690.49	80.35	0.26	0.02
Univariate	116.95	14.17	0.09	0.00	117.78	16.34	0.09	0.01
Multivariate	123.81	17.95	0.09	0.00	127.75	23.12	0.09	0.01
Proposed	12.16	2.76	0.08	0.01	**17.09**	2.25	0.09	0.02
Discharge[1]	164.25	59.21	0.09	0.01	206.16	55.69	0.11	0.01
Variance[1]	266.53	40.14	0.12	0.01	276.77	88.44	0.13	0.02
Variance-M	60.53	11.72	0.08	0.00	52.69	24.13	**0.08**	0.01
GRNN[2]	20.57	20.62	**0.04**	0.03	73.14	38.68	0.11	0.02
Random Forest Regression	**8.54**	1.49	**0.04**	0.01	22.45	4.51	0.09	0.02

1. For Discharge model, the original model uses minimum value of ΔQ100-10(V), variance of ΔQ100-10(V), skewness of ΔQ100-10(V), kurtosis of ΔQ100-10(V), the discharge capacity at cycle 2, and the difference between max discharge capacity and cycle 2 [8]. In this study, due to different dataset, the features are modified as following: minimum value of ΔQ5-1(V), variance of ΔQ5-1(V), skewness of ΔQ5-1(V), kurtosis of ΔQ5-1(V), the discharge capacity at cycle 2, and the difference between max discharge capacity and cycle 2.

2.For Variance model, the variance of ΔQ5-1(V) is used.

3. For Variance-M model, three features are used: 1) variance of ΔQ5-1(V), 2) prospective cumulative faraday efficiency, 3) average capacity fading rate for the past 5 cycles, ξ_5.

4. For the GRNN model, the original model uses variance of ΔQ100-10(V), skewness of ΔQ100-10(V), the fitting slope of the 2nd to 100th cycle discharge capacity curve, and the internal resistance difference between 100^{th} and 2^{nd} cycle [14]. However, due to the different dataset, the features are modified as follows: (1) variance of ΔQ5-1(V), (2) skewness of ΔQ5-1(V), and (3) the fitting slope of the 1^{st} to 5^{th} cycle discharge capacity curve.